

## Minimizing the linewidth of the flux-flow oscillator

Andrey L. Pankratov<sup>a)</sup>

*Institute for Physics of Microstructures of RAS, Nizhny Novgorod 603950, Russia*

(Received 30 October 2007; accepted 12 January 2008; published online 26 February 2008)

The linewidth of the flux-flow oscillator has been calculated by direct computer simulation of the sine-Gordon equation with noise. Good agreement of the numerical results with the formula derived in Phys. Rev. B **65**, 054504 (2002) has been achieved. Depending on the length of the unbiased tail, the power may be maximized and the linewidth may be minimized in a broad range of bias currents. The linewidth can be decreased further by 1.5 times by proper load matching. © 2008 American Institute of Physics. [DOI: 10.1063/1.2839605]

During the last decade, the flux-flow oscillator (FFO), based on a viscous flow of magnetic flux quanta in a long Josephson tunnel junction (JTT),<sup>1</sup> has emerged as the most promising local oscillator for superconducting spectrometers.<sup>2</sup> Its wide operational bandwidth and easy broadband tunability make it attractive for both space-borne radio astronomy and atmospheric monitoring. However, the spectral linewidth of the emitted radiation of the free-running FFO is rather large, which complicates phase locking. Typically, the free-running linewidth is 2–20 MHz for an Nb–AlO<sub>x</sub>–Nb FFO in the 400–700 GHz frequency range. For spectral applications, it is of crucial importance to reduce the FFO linewidth to make it more uniform in all working frequency range and to increase the emitted power to improve the signal-to-noise ratio.

The dynamical properties of the FFO were investigated in Refs. 1–18. In particular, linewidth was studied both experimentally<sup>7–11</sup> and theoretically.<sup>12–16</sup> However, only one formula for the linewidth<sup>15</sup> takes into account the differential resistance as a function of both the bias current and the magnetic field. It has proven to adequately describe experimental results.<sup>10,11</sup> Still, the conversion of bias current fluctuations to magnetic field fluctuations is unclear. Also, the dependence of the linewidth on the bias current profile and certain parameters, such as *RC* load, has not been systematically studied yet, either theoretically or experimentally.

The aim of the present paper is to study the FFO linewidth by direct computer simulation of the sine-Gordon equation with noise and to make certain optimizations of FFO design in order to minimize the linewidth and to increase the emitted power.

For several decades the sine-Gordon equation has been the most adequate model for the long JTT, giving a good qualitative description of its basic properties

$$\phi_{tt} + \alpha\phi_t - \phi_{xx} = \beta\phi_{xxt} + \eta(x) - \sin(\phi) + \eta_f(x,t), \quad (1)$$

where indices *t* and *x* denote temporal and spatial derivatives. Space and time are normalized to the Josephson penetration length  $\lambda_J$  and to the inverse plasma frequency  $\omega_p^{-1}$ , respectively,  $\alpha = \omega_p/\omega_c$  is the damping parameter,  $\omega_p = \sqrt{2eI_c/\hbar C}$ ,  $\omega_c = 2eI_c R_N/\hbar$ ,  $I_c$  is the critical current,  $C$  is the JTT capacitance,  $R_N$  is the normal state resistance,  $\beta$  is the surface loss parameter,  $\eta(x)$  is the dc overlap bias current density, normalized to the critical current density  $J_c$ , and

$\eta_f(x,t)$  is the fluctuational current density. If the critical current density is fixed and the fluctuations are treated as white Gaussian noise with zero mean, its correlation function is  $\langle i_f(x,t)i_f(x',t') \rangle = 2\alpha\gamma\delta(x-x')\delta(t-t')$ , where  $\gamma = I_T/(J_c\lambda_J)$  is the dimensionless noise intensity,<sup>18</sup>  $I_T = 2ekT/\hbar$  is the thermal current,  $e$  is the electron charge,  $\hbar$  is the Planck constant,  $k$  is the Boltzmann constant, and  $T$  is the temperature.

The boundary conditions that simulate simple *RC* loads, see Refs. 3 and 17, have the form

$$\begin{aligned} \phi(0,t)_x + r_L c_L \phi(0,t)_{xt} - c_L \phi(0,t)_{tt} + \beta r_L c_L \phi(0,t)_{xtt} \\ + \beta \phi(0,t)_{xt} = \Gamma - \Delta\Gamma, \end{aligned} \quad (2)$$

$$\begin{aligned} \phi(L,t)_x + r_R c_R \phi(L,t)_{xt} + c_R \phi(L,t)_{tt} + \beta r_R c_R \phi(L,t)_{xtt} \\ + \beta \phi(L,t)_{xt} = \Gamma + \Delta\Gamma. \end{aligned} \quad (3)$$

Here,  $\Gamma$  is the normalized magnetic field,  $\Delta\Gamma = 0.05\Gamma$ , see Ref. 17, and  $L$  is the dimensionless length of JTT. The dimensionless capacitances and resistances  $c_{L,R}$  and  $r_{L,R}$  are the FFO *RC* load placed at the left (output) and at the right (input) ends, respectively. Following Ref. 16, if both the overlap  $\eta_{ov} = (1/L)\int_0^L \eta(x)dx$  and the inline  $\eta_{in} = 2\Delta\Gamma/L$  components of the current are present, the total current  $\eta_t$  with respect to which all current-voltage characteristics (IVCs) will be computed, is the sum of overlap and inline components  $\eta_t = \eta_{ov} + \eta_{in}$ .

In Ref. 17 on the basis of the same model (1)–(3) without the noise term, the investigation of current-voltage characteristics of FFO was performed. For the bias current profile, depicted in the inset of Fig. 1 by curve with crosses, good qualitative agreement with experimental IVCs was achieved. Due to experimental motivation the current profile was parabolic (with the curvature  $a = 0.005$ ) between the left and the right boundaries of bias electrode  $x_0$  and  $x_1$  ( $0 \leq x_0 \leq x_1 \leq L$ ), and dropped down exponentially in the unbiased tails  $x \leq x_0$ ,  $x \geq x_1$ :  $\exp(-px)$  (with  $p = 0.13$  in Fig. 1).

In Ref. 1, it was suggested to use the unbiased tail for decreasing the differential resistance  $r_d = dv/d\eta_t$ . This might reduce the linewidth, provided the formula for the linewidth of short JTT (Ref. 19) worked for FFO (here and below the linewidth is defined as full width half power),  $\Delta f_s = 2\alpha\gamma r_d^2/L$ . Later, it was found experimentally<sup>9</sup> that even for small  $r_d$  the FFO linewidth is almost one order of magnitude larger than predicted by the formula for short JTT. The for-

<sup>a)</sup>Electronic mail: alp@ipm.sci-nnov.ru.

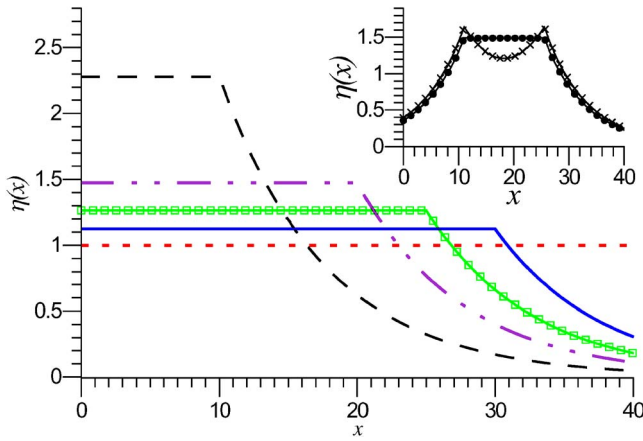


FIG. 1. (Color online) The distribution of overlap component of bias current  $\eta(x)$ . Short-dashed line,  $\eta(x) = \eta_0$ ; solid curve,  $x_1 = 30$ ; curve with rectangles,  $x_1 = 25$ ; dot-dashed curve,  $x_1 = 20$ ; long-dashed curve,  $x_1 = 10$ . Inset: curve with circles,  $x_0 = 11$ ,  $x_1 = 25.5$ ,  $a = 0$ ; curve with crosses,  $x_0 = 11$ ,  $x_1 = 25.5$ ,  $a = 0.005$ .

mula for the FFO linewidth of Ref. 15, which in addition to  $r_d$  takes into account differential resistance over magnetic field  $r_d^{CL} = Ldv/d\Gamma$

$$\Delta f_{\text{FFO}} = 2\alpha\gamma(r_d + \sigma r_d^{CL})^2/L \quad (4)$$

demonstrates good agreement with experiment.<sup>10,11</sup> In Ref. 6, it has been shown that it is desirable to supply more bias current at the radiating end than at the input end to enhance the radiation. Therefore, in the frame of the present paper we shift the current profile to the left,  $x_0 = 0$ , and vary the length of unbiased tail, which is located at the right end of J TJ. Also, to avoid problems with the scaling of parabolic curvature, let us set the current profile to be constant between  $x_0$  and  $x_1$ .

The power at RC load at the radiating end  $x=0$  for different bias current profiles depicted in Fig. 1 is presented in Fig. 2. The power is computed in accordance with Ref. 3. The implicit difference scheme, used to solve Eq. (1) with noise, was tested in Ref. 18. The parameters are as follows:  $L=40$ ,  $\alpha=0.033$ ,  $\beta=0.035$ ,  $c_L=c_R=100$ ,  $r_L=2$ ,  $r_R=100$ ,  $\Gamma=3.6$ , and  $\gamma=0.1$ . From Fig. 2, one can see that the current

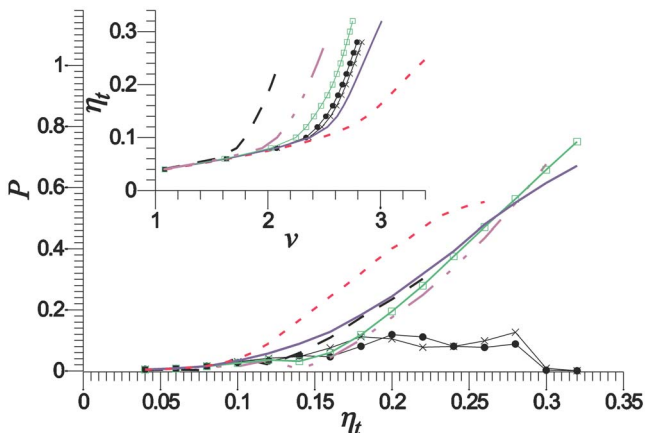


FIG. 2. (Color online) Radiated power vs total current, computed for  $\eta(x)$ , presented in Fig. 1: short-dashed curve,  $\eta(x) = \eta_0$ ; solid curve,  $x_1 = 30$ ; curve with rectangles,  $x_1 = 25$ ; dot-dashed curve,  $x_1 = 20$ ; long-dashed curve,  $x_1 = 10$ ; curve with circles,  $x_0 = 11$ ,  $x_1 = 25.5$ ,  $a = 0$ ; curve with crosses,  $x_0 = 11$ ,  $x_1 = 25.5$ ,  $a = 0.005$ . Inset: dc current-voltage characteristics computed for  $\eta(x)$ , presented in Fig. 1, the notations are the same as for power.

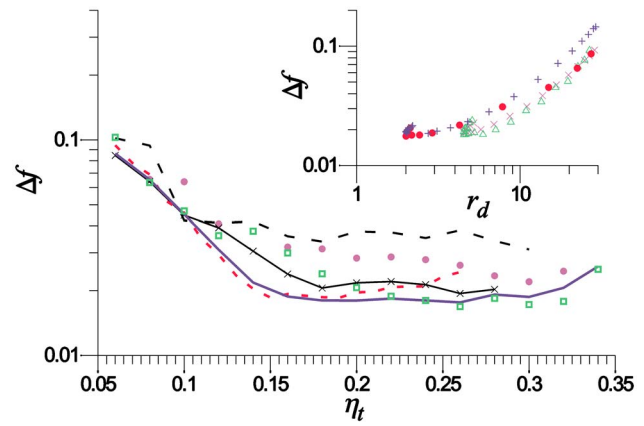


FIG. 3. (Color online) FFO linewidth vs total current for  $\eta(x)$  from Fig. 1,  $\gamma=0.1$ : short-dashed curve,  $\eta(x) = \eta_0$ ; solid curve,  $x_1 = 30$ ; rectangles,  $x_1 = 25$ ; circles,  $x_1 = 20$ ; long-dashed curve,  $x_1 = 10$ ; curve with crosses,  $x_0 = 11$ ,  $x_1 = 25.5$ ,  $a = 0.005$ . Inset: FFO linewidth versus differential resistance. Triangles and crosses – simulations and theory (4),  $\sigma = 0.185$ , for homogeneous bias current distribution; circles and daggers – simulations and theory,  $\sigma = 0.24$ , for the case with unbiased tail  $x_1 = 30$ .

profile with one unbiased tail  $x_1 = 25$  gives maximal power among all the considered current profiles. For the case of two unbiased tails  $x_0 = 11$  and  $x_1 = 25.5$ , the power is minimal and almost one order of magnitude smaller than for  $x_1 = 25$ . In the inset of Fig. 2, the current-voltage characteristics for the same current profiles are given for comparison. The flux-flow steps have the largest height also for  $x_1 = 25$ . The height of IVCs for both profiles with  $x_0 = 11$ ,  $x_1 = 25.5$  and  $a = 0.005$ ,  $a = 0$  have close values to each other and are comparable to  $x_1 = 25$ . So, it is desirable to apply larger bias current at the radiating end to get higher emitted power.

The power spectral density of FFO is computed as Fourier transform of the correlation function of the second kind  $\Phi(\tau) = (1/T_{\text{av}}) \int_0^{T_{\text{av}}} \langle v_0(t)v_0(t+\tau) \rangle dt$ , where  $v_0(t) = d\varphi(t)/dt$  is the voltage at the RC load ( $x=0$ ) and  $T_{\text{av}}$  is the averaging time. There are two general restrictions complicating the calculation of the spectral density. On the one hand, the time step should be small enough to resolve oscillations and on the other hand the averaging time  $T_{\text{av}}$  should be rather large to resolve fine spectral spikes. Due to these restrictions, the noise intensity was chosen  $\gamma=0.1$ . Nevertheless, this is the same limit of low noise intensity as in experiments, since IVCs are almost unaffected by the noise, the spectral spikes are narrow, and the linewidth perfectly scales proportionally to the noise intensity (see below).

The emitted signal of FFO at flux-flow steps is nearly sinusoidal, in agreement with Ref. 3 and experimental results. The power contained in the second and third harmonics is much lower than in the main one, containing about 99% of the total power.<sup>20</sup> Also, the spectral peak is perfectly Lorentzian in more than two orders of magnitude interval. This is quite different with spectral densities at the displaced linear slope, i.e., at small bias currents and magnetic fields, where chaotic behavior is possible and the linewidth is extremely large.<sup>8</sup>

The comparison of the computer simulation results with formula (4) is presented in the inset of Fig. 3 and the agreement is rather good. However, the considered model is one-dimensional and the only bias current is fluctuating, so the reasoning of Refs. 15 and 16 about nature of magnetic field fluctuations is not fully adequate. The conversion of bias

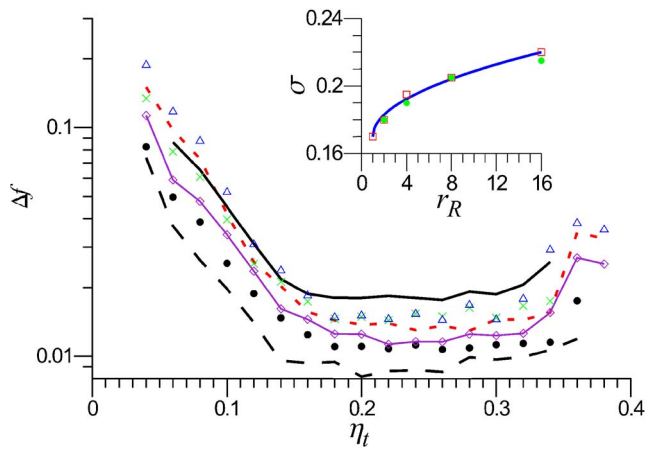


FIG. 4. (Color online) FFO linewidth vs total current computed for different values of load resistances and noise intensity,  $x_1=30$ : solid curve,  $r_L=2$ ,  $r_R=100$ ; triangles,  $r_L=r_R=8$ ; crosses,  $r_L=2$ ,  $r_R=8$ ; short-dashed curve,  $r_L=r_R=4$ ; curve with diamonds,  $r_L=r_R=2$ ; circles,  $r_L=r_R=1$ ; all these curves for  $\gamma=0.1$ ; long-dashed curve,  $r_L=2$ ,  $r_R=100$  for  $\gamma=0.05$ . Inset: the coefficient  $\sigma$  vs  $r_R$ , rectangles,  $r_L=r_R$ ; circles,  $r_L=2$ ; solid curve, fitting  $\sqrt{r_R}$ .

current fluctuations to magnetic field fluctuations may be explained by the noise self-pumping effect: fluctuating fluxons, radiating from the FFO, induce fluctuating magnetic field, which in turn modulates the fluxon dynamics and increases the linewidth. To see how the linewidth behaves in the whole working range, let us plot it versus the total bias current  $\eta_t$ .

Let us analyze the dependence of the linewidth on the length of the unbiased tail. From Fig. 3, it is seen that minimal value of  $\Delta f$  is reached for several cases, including the case of  $\eta(x)=\eta_0$ . However, for the unbiased tail  $x_1=30$ , the linewidth is nearly constant (and minimal) in the maximal range of bias currents. So, the unbiased tail of  $1/4$  of junction length, giving nearly maximal power and nearly minimal linewidth in the broadest range of bias current, can be recommended for spectral applications.

Normally, FFO radiating end  $x=0$  is well matched to the external environment, while the opposite end is strongly mismatched, as it was modeled in Ref. 17 and in the present paper. It is interesting to analyze how the linewidth will change, if the FFO is better matched at both ends. The results of this analysis are presented in Fig. 4 for  $x_1=30$ . It can be seen, that improved matching at the opposite end decreases the linewidth by 1.5 times. It is important to note that equal matching at both ends gives smaller linewidth than perfect matching at the radiating end and bad at the opposite one, e.g., compare the curves for  $r_L=2$ ,  $r_R=100$  and  $r_L=r_R=4$  and note that the curves for  $r_L=r_R=8$  and  $r_L=2$ ,  $r_R=8$  nearly coincide. The lowest curve is computed for noise intensity

$\gamma=0.05$  and the linewidth is two times smaller than for  $\gamma=0.1$ , confirming that we are indeed in the low noise limit, and the corresponding curves for smaller noise intensity can be obtained by scaling. Finally, it is important to mention that the noise conversion factor  $\sigma$  perfectly scales as  $\sqrt{r_R}$  both for  $r_L=2$ , and for  $r_L=r_R$ .

The linewidth of flux-flow oscillator has been calculated by numerical solution of the modified sine-Gordon equation with noise that takes into account surface losses and  $RC$  load. Good agreement of the computer simulation results with formula (4) has been achieved. Varying the length of the unbiased tail, the power may be maximized and the linewidth may be minimized in a broad range of bias currents. The linewidth can be decreased further by 1.5 times by proper load matching.

The author wishes to thank V. P. Koshelets and J. Mygind for discussions and constructive comments. The work was supported by ISTC project 3174.

- <sup>1</sup>T. Nagatsuma, K. Enpuku, F. Irie, and K. Yoshida, *J. Appl. Phys.* **54**, 3302 (1983), see also **56**, 3284 (1984); **58**, 441 (1985); **63**, 1130 (1988).
- <sup>2</sup>V. P. Koshelets and S. V. Shitov, *Supercond. Sci. Technol.* **13**, R53 (2000).
- <sup>3</sup>C. Soriano, G. Costabile, and R. D. Parmentier, *Supercond. Sci. Technol.* **9**, 578 (1996).
- <sup>4</sup>M. Cirillo, N. Grønbech-Jensen, M. R. Samuelsen, M. Salerno, and G. V. Rinati, *Phys. Rev. B* **58**, 12377 (1998).
- <sup>5</sup>M. Salerno and M. R. Samuelsen, *Phys. Rev. B* **59**, 14653 (1999).
- <sup>6</sup>A. L. Pankratov, *Phys. Rev. B* **66**, 134526 (2002).
- <sup>7</sup>V. P. Koshelets, A. Shchukin, I. L. Lapytskaya, and J. Mygind, *Phys. Rev. B* **51**, 6536 (1995).
- <sup>8</sup>A. V. Ustinov, H. Kohlstedt, and P. Henne, *Phys. Rev. Lett.* **77**, 3617 (1996).
- <sup>9</sup>V. P. Koshelets, S. V. Shitov, A. V. Shchukin, L. V. Filippenko, J. Mygind, and A. V. Ustinov, *Phys. Rev. B* **56**, 5572 (1997).
- <sup>10</sup>V. P. Koshelets, P. N. Dmitriev, A. B. Ermakov, A. S. Sobolev, A. M. Baryshev, P. R. Wesselius, and J. Mygind, *Supercond. Sci. Technol.* **14**, 1040 (2001).
- <sup>11</sup>V. P. Koshelets, P. N. Dmitriev, A. S. Sobolev, A. L. Pankratov, V. V. Khodos, V. L. Vaks, A. M. Baryshev, P. R. Wesselius, and J. Mygind, *Physica C* **372-376**, 316 (2002).
- <sup>12</sup>A. A. Golubov, B. A. Malomed, and A. V. Ustinov, *Phys. Rev. B* **54**, 3047 (1996).
- <sup>13</sup>A. P. Betenev and V. V. Kurin, *Phys. Rev. B* **56**, 7855 (1997).
- <sup>14</sup>M. Salerno, M. R. Samuelsen, and A. V. Yulin, *Phys. Rev. Lett.* **86**, 5397 (2001).
- <sup>15</sup>A. L. Pankratov, *Phys. Rev. B* **65**, 054504 (2002).
- <sup>16</sup>J. Mygind, V. P. Koshelets, M. Samuelsen, and A. S. Sobolev, *IEEE Trans. Appl. Supercond.* **15**, 968 (2005).
- <sup>17</sup>A. L. Pankratov, A. S. Sobolev, V. P. Koshelets, and J. Mygind, *Phys. Rev. B* **75**, 184516 (2007).
- <sup>18</sup>K. G. Fedorov and A. L. Pankratov, *Phys. Rev. B* **76**, 024504 (2007).
- <sup>19</sup>K. K. Likharev, *Dynamics of Josephson Junctions and Circuits* (Gordon and Breach, New York, 1986); A. Barone and G. Paterno, *Physics and Applications of the Josephson Effect* (Wiley, New York, 1982).
- <sup>20</sup>A. L. Pankratov, arXiv:0707.1413v1 [cond-mat.supr-con].